



Technical note: Do different projections matter for the Budyko framework?

Remko C. Nijzink and Stanislaus J. Schymanski

Catchment and Ecohydrology Group (CAT), Environmental Research and Innovation (ERIN),
Luxembourg Institute of Science and Technology (LIST), Belvaux, Luxembourg

Correspondence: Remko C. Nijzink (remko_nijzink@live.nl)

Received: 6 April 2022 – Discussion started: 20 April 2022

Revised: 12 July 2022 – Accepted: 20 August 2022 – Published: 14 September 2022

Abstract. The widely used Budyko framework defines the water and energy limits of catchments. Generally, catchments plot close to these physical limits, and Budyko (1974) developed a curve that predicted the positions of catchments in this framework. Often, the independent variable is defined as an aridity index, which is used to predict the ratio of actual evaporation over precipitation (E_a/P). However, the framework can be formulated with the potential evaporation as the common denominator for the dependent and independent variables, i.e., P/E_p and E_a/E_p . It is possible to mathematically convert between these formulations, but if the parameterized Budyko curves are fit to data, the different formulations could lead to differences in the resulting parameter values. Here, we tested this for 357 catchments across the contiguous United States.

In this way, we found that differences in n values due to the projection used could be ± 0.2 . If robust fitting algorithms were used, the differences in n values reduced but were nonetheless still present. The distances to the curve, often used as a metric in Budyko-type analyses, systematically depended on the projection, with larger differences for the non-contracted sides of the framework (i.e., $E_p/P > 1$ or $P/E_p > 1$). When using the two projections for predicting E_a , we found that uncertainties due to the projections used could exceed 1.5 %. An important reason for the differences in n values, curves and resulting estimates of E_a could be found in data points that clearly appear as outliers in one projection but less so in the other projection.

We argue here that the non-contracted side of the framework in the two projections should always be assessed, especially for data points that appear as outliers. At least, one

should consider the additional uncertainty of the projection and assess the robustness of the results in both projections.

1 Introduction

Budyko (1974) defined the water and energy limits of catchments in a simple framework and found that most catchments plot close to these limits. He defined a curve through these observations, which is known as the Budyko curve. The framework and curve are widely applied, and the original work of Budyko (1974) has been cited over 3100 times (Google Scholar). Besides that, Budyko's approach finds itself currently in a renaissance, as can be noted by the large number of studies related to the Budyko framework over the recent years. The strength of the approach is widely acknowledged, and especially its simplicity is appealing.

Even though often referred to as the Budyko framework, the base of the framework was formed by the work of Ol'Dekop (1911) and Schreiber (1904). Initially, Schreiber (1904) formulated an exponential function to calculate the runoff ratio of a catchment but only as a function of precipitation and a constant, catchment-specific parameter. Ol'Dekop (1911) added evaporation to this equation but also formulated his own hyperbolic tangent function. Budyko (1974) took later the arithmetic mean of the exponential function and the hyperbolic tangent function, which both had no parameters, to adjust the curve. This was changed by Turc (1954) in France and independently in the Soviet Union by Mezentsev (1955), who both introduced an adjustable exponent. This parameterized form was adopted later by others, in more general formulations, e.g., Fu (1981), Zhang et al. (2001), and

Roderick and Farquhar (2011). These formulations often use one single parameter to adjust the curve to the observations. See also Andréassian and Sari (2019) for more details about the historical perspective.

More recently, the Budyko framework has gained popularity with several studies that use the framework for water balance assessment (e.g., Andréassian and Perrin, 2012; Coron et al., 2015), model constraining (e.g., Nijzink et al., 2018; Hulsman et al., 2018; Mianabadi et al., 2019; Greve et al., 2020) or the assessment of climate change effects (e.g., van der Velde et al., 2014; Bouaziz et al., 2022). In addition, several studies exist that adjust the framework for different timescales (Zhao et al., 2020; Wang et al., 2022) or different application fields (Sankarasubramanian et al., 2020).

A large number of studies consider the parameter in the Budyko framework to be catchment-specific and a function of local catchment characteristics. It has been argued that this parameter explains local climatic and environmental conditions combined (e.g., Roderick and Farquhar, 2011), but it is often also related to vegetation (e.g., Yang et al., 2009; Li et al., 2013; Ning et al., 2017), land cover (Oudin et al., 2008) or human activities (Liang et al., 2015; Yang et al., 2020). Moreover, Zhang et al. (2001) defined n specifically as the plant-available water coefficient. In addition to vegetation, Donohue et al. (2012) related the parameter to multiple variables including storm depths and soil water storage capacities. Furthermore, seasonality is often considered as well as a factor that influences this parameter (Shao et al., 2012; Ning et al., 2017).

Budyko formulated his curve with an aridity index as the independent variable, and most other publications followed that definition. From the older and traditionally cited publications, only Turc (1954) and Pike (1964) formulated the framework with potential evaporation as the common denominator and P/E_p as the independent variable (Andréassian et al., 2016). Nowadays, most publications still use a form of the Budyko framework with the dryness or aridity index E_p/P to predict the dependent variable E_a/P , similar as Budyko, but a substantial number of papers use P/E_p as an independent variable to predict the ratio of E_a/E_p . Here we refer to these different ways of expressing the dependent and independent variables in the Budyko framework as dryness index and wetness index projections, respectively. These two projections are only discussed in combination in very few studies (e.g., Moussa and Lhomme, 2016; Porporato, 2022).

The choice of the projection may depend on the purpose of a given study. Often, the projection with an aridity index is used as it allows for a straightforward estimation of the runoff ratio ($Q/P = 1 - E_a/P$), which can, for example, be used directly for constraining hydrological models (e.g., Nijzink et al., 2018; Hulsman et al., 2018). In contrast, assessing responses to changes in precipitation may require a projection that uses E_a/E_p as the predicted variable (e.g., Dooge et al., 1999), in order to allow for a clearer interpretation of sensitivities. Others use the different pro-

jections simultaneously, for example, to identify gaining or leaky catchments (Andréassian and Perrin, 2012). However, a large number of studies use the projection based on an aridity index, most likely just following the definition of the framework by Budyko (1974), without questioning the appropriateness of this projection.

Generally, the projections should not make a large difference, as the equations can be rewritten in the different formats (see, for example, Roderick and Farquhar, 2011), but here we argue that this does matter in case the curve is fit to observations. Moreover, these different ways of defining the Budyko space may lead to different interpretations of deviations from the curve. Therefore, we explore here the consequences of the projection used and address the following research question: does the choice of the projection and fitting algorithm have a systematic influence on the curve parameter, uncertainties, distances of individual catchments to the curve or distances of individual catchments to the physical limits?

2 Methodology

In order to address the research question, the Budyko framework was applied to a selection of catchments across the contiguous United States. An open science approach was followed using the platform Renku (<https://renkulab.io/>, last access: 30 March 2022), which stores all data, scripts and analyses as well as the linkage between these elements. An online repository contains all information necessary for reproducibility and repeatability (<https://renkulab.io/projects/remko.nijzink/budyko>; Nijzink and Schymanski, 2022b), with the final figures and latex files in a separate repository (https://renkulab.io/gitlab/remko.nijzink/budyko_tech_note, last access: 4 April 2022).

2.1 Budyko formulations

The Budyko formulation adopted for our analysis was originally formulated by Mezentsev (1955) (as traced back by Yang et al., 2008) but used afterwards by, amongst others, Choudhury (1999) and Roderick and Farquhar (2011):

$$\overline{E_a} = \frac{\overline{E_p} \overline{P}}{\left(\overline{P}^n + \overline{E_p}^n\right)^{1/n}}, \quad (1)$$

with $\overline{E_p}$ the mean annual potential evaporation, $\overline{E_a}$ the mean annual evaporation, \overline{P} the mean annual precipitation and n a shape factor, assumed to represent catchment characteristics (e.g., vegetation, soils). This equation can be reformulated by dividing the left-hand side and right-hand side by \overline{P} , followed by dividing the nominator and denominator on the right-hand side by \overline{P} as well, leading to

$$\frac{\overline{E_a}}{\overline{P}} = \frac{\overline{E_p}}{\overline{P}} \left(\left(\frac{\overline{E_p}}{\overline{P}} \right)^n + 1 \right)^{-1/n}. \quad (2)$$

Table 1. Loss functions used for fitting the Budyko curves, from https://docs.scipy.org/doc/scipy/reference/generated/scipy.optimize.curve_fit.html, last access: 10 February 2022.

Method	Equation
Linear	$\rho(z) = z$
Soft	$\rho(z) = 2 \cdot ((1+z)^{0.5} - 1)$
Huber	$\rho(z) = \begin{cases} z, & \text{if } z \leq 1. \\ 2 \cdot z^{0.5} - 1, & \text{otherwise.} \end{cases}$
Cauchy	$\rho(z) = \ln(1+z)$
Arctan	$\rho(z) = \arctan(z)$

In a similar way, Eq. (1) can be expressed by the ratio of \bar{P}/\bar{E}_p as the dependent variable. First, both sides of Eq. (1) are divided by \bar{E}_p again, followed by dividing the nominator and denominator on the right-hand side by \bar{E}_p (see also Supplement S1):

$$\frac{\bar{E}_a}{\bar{E}_p} = \frac{\bar{P}}{\bar{E}_p} \left(\left(\frac{\bar{P}}{\bar{E}_p} \right)^n + 1 \right)^{-1/n}. \quad (3)$$

These two formulations are often used interchangeably, and data can be plotted in figures based on Eqs. (2) or (3). We will adopt here dryness index projection and wetness index projection throughout the paper for projections based on Eqs. (2) and (3), respectively, to refer to these different ways of applying the Budyko framework.

2.2 Fitting the Budyko equations

The exponent n in Eqs. (2) and (3) was fit to data of multiple catchments with a least-squares fit based on the Levenberg–Marquardt algorithm (python `scipy.optimize.curve_fit`, https://docs.scipy.org/doc/scipy/reference/generated/scipy.optimize.curve_fit.html, last access: 10 February 2022, Levenberg, 1944). Normally, this algorithm minimizes the sum of the squared residuals; i.e., it uses a linear least-squares loss function. Afterwards, instead of using a linear least-squares loss function, other loss functions to minimize the residuals were used, in order to obtain a robust fit. These loss functions $\rho(z)$ are summarized in Table 1, and the final, resulting loss function is defined as

$$\rho' = C^2 \cdot \rho(x_r^2/C^2), \quad (4)$$

with x_r the residual of data point x , C a scale parameter, ρ' the resulting loss and $\rho()$ the loss function (see Table 1). The scale parameter C generally separates outliers from the data and was given different values between 0.1 and 1 in order to vary the data points that are considered as outliers, where low values of C classify the most data points as outliers. Note that $C = 1$ with a linear loss function results in an ordinary least-squares fit again.

2.3 CAMELS data

In order to test the different hypotheses, the CAMELS data (Addor et al., 2017; Newman et al., 2015) were used, as they provide a large dataset of 671 catchments across the contiguous United States. For each catchment in this dataset, daily discharge, rainfall, potential evaporation and air temperature are available. Eventually, 357 catchments were selected based on several conditions similar to Gnann et al. (2019).

- positive long-term mean discharge: $\bar{Q} \geq 0 \text{ mm yr}^{-1}$
- positive long-term mean precipitation: $\bar{P} \geq 0 \text{ mm yr}^{-1}$
- runoff ratio smaller than unity: $\bar{Q}/\bar{P} \leq 1$
- long-term actual evaporation not exceeding potential evaporation: $1 - \bar{Q}/\bar{P} \leq \bar{E}_p/\bar{P}$
- no lakes: water fraction $\geq 5 \%$
- no snow-dominated catchments: mean elevation $\leq 2000 \text{ m}$ and snow days $\leq 20 \%$
- relatively large catchments: area $\geq 100 \text{ km}^2$.

Afterwards, the actual evaporation was determined based on the long-term water balance, assuming that storage change is negligible over a longer period of time:

$$\bar{E}_a = \bar{P} - \bar{Q}, \quad (5)$$

with \bar{P} the mean annual precipitation, \bar{Q} the mean annual discharge and \bar{E}_a the mean annual actual evaporation. In this way, all water balance components are known to plot the data in the Budyko space.

2.4 Approach

The research question was addressed by a simple approach. First, the Budyko curves were fit to the CAMELS data with the different loss functions as defined in Sect. 2.2, in the two different projections. This was done for the selected 357 catchments all together, as well as for catchments grouped by a high aridity ($\bar{E}_p/\bar{P} > 1$, 247 catchments) and a low aridity ($\bar{E}_p/\bar{P} \leq 1$, 110 catchments), the latter to assess whether differences start to occur when catchments are dominantly in either the contracted side of the framework (i.e., $\bar{E}_p/\bar{P} \leq 1$ or $\bar{P}/\bar{E}_p \geq 1$) or the non-contracted side of the framework. The vertical distances to the curve as well as the distances to the envelope of the physical limits were calculated for the different projections.

In the next step, the uncertainty in the estimated mean annual actual evaporation due to the different projections was assessed. This was done by selecting one catchment for the prediction of mean annual actual evaporation, whereas the remaining 356 catchments were used to fit the Budyko curve. This was again carried out in a projection based on a wetness

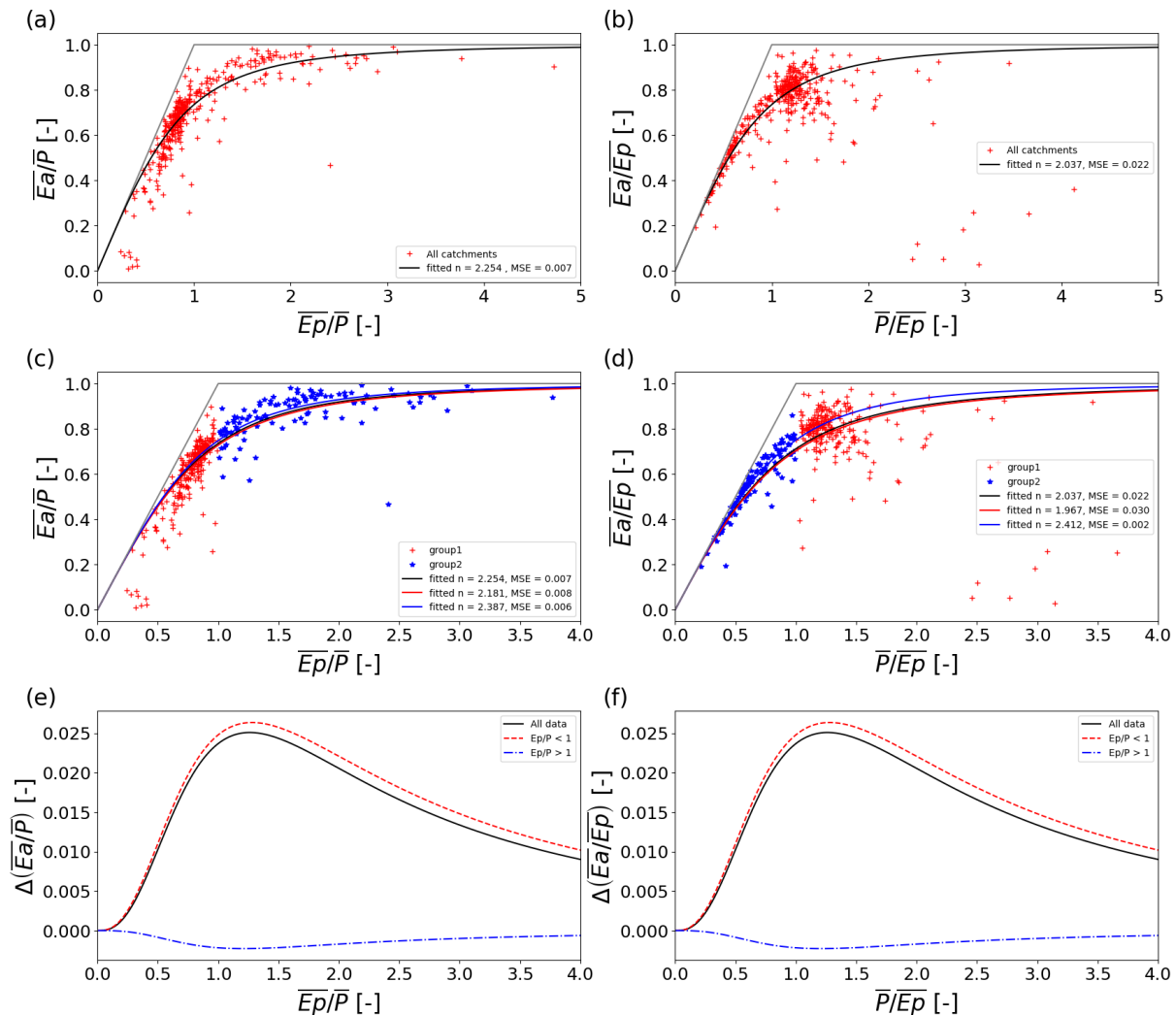


Figure 1. CAMELS dataset plotted in different projections of the Budyko space, with (a) and (c) a projection normalized by precipitation for all catchments and (b), and (d) a projection normalized by potential evaporation. In (c) and (d) the catchments are split into two groups that are either water-limited or energy-limited, with the best fit curve for all catchments in black, the best fit for the group of energy-limited catchments in red and the best fit for the group of water-limited catchments in blue. The differences between the curves in (c) and (d) are shown in (e) for a projection normalized by precipitation, whereas (f) shows the differences between the curves in (c) and (d) for a projection normalized by potential evaporation.

index and a dryness index. As both estimates can be considered equally likely, the uncertainty was defined as the relative difference from the mean of the two estimates (i.e., the difference between the estimates equals 2 times the uncertainty). In addition, the predictions were evaluated by the relative error compared with the water balance based observed evaporation. The procedure was repeated for each catchment, leading to uncertainty estimates and relative errors for each catchment. Eventually, predictions were also made by just using the non-contracted side of the framework.

3 Results and discussion

3.1 Fitting the Budyko curve for different projections

Fitting the selected catchments of the CAMELS dataset to the two different projections led to different values for the n exponent in Eqs. (2) and (3) (Fig. 1a and b, $n = 2.254$ and $n = 2.037$, respectively). These n values differed even stronger when the catchments were separated into two groups based on their aridity ($E_p/P > 1$ and $E_p/P \leq 1$, respectively, Fig. 1c and d). In particular, for the energy-limited catchments ($E_p/P \leq 1$, shown in red), the values changed strongly from an n value of 2.181 in the projection with a dryness index (Fig. 1c) to a value of 1.967 in the projec-

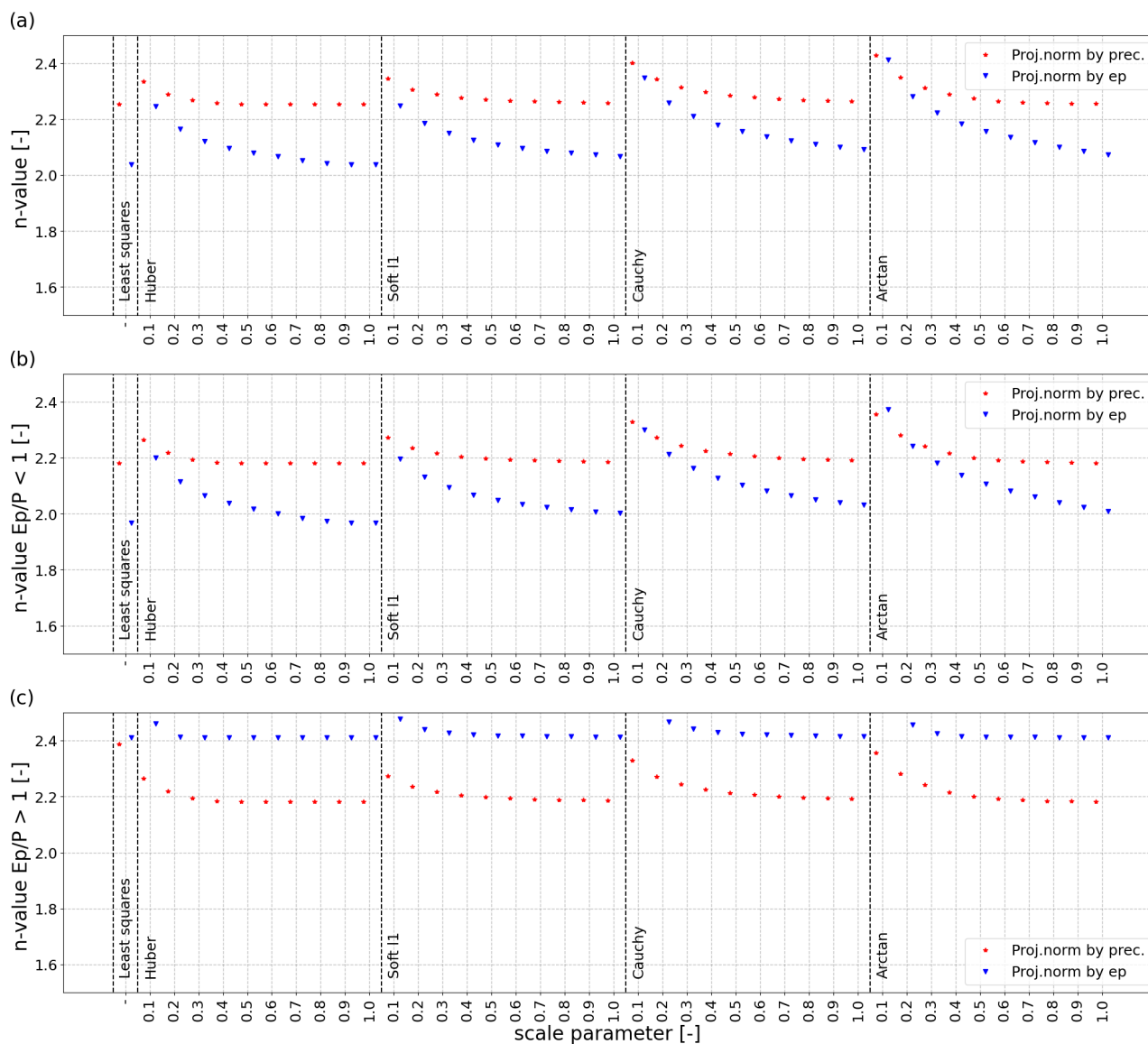


Figure 2. Fitted n values for (a) all catchments, (b) energy-limited catchments and (c) water-limited catchments, for projections that normalized by precipitation (blue) and potential evaporation (red). On the x axis, the different robust regression methods with different scale parameters (separating outliers from the data) are shown.

tion with a wetness index (Fig. 1d). The differences that occurred when the curves with the two different n values from the two different projections were used in the same projection and subtracted from each other (Fig. 1e and f) also show that especially the curves based on energy-limited catchments strongly deviated ($E_p/P \leq 1$, shown in red). In contrast, the curves obtained for water-limited catchments ($E_p/P > 1$, blue) remained more similar, with negligible differences.

The results presented in Fig. 1 also strongly depended on the choice of the method, which was here a linear least-squares fit. Repeating the analysis with more robust methods (see Table 1) led to smaller differences between n val-

ues in the two projections, even though differences were still present (Fig. 2a). In particular, the scale parameter C (Eq. 4) that identifies data points as outliers had a strong effect on the resulting n values when set to a larger value. Nevertheless, differences still occurred for small values of this scale parameter, i.e. the most stringent values that classify the most data points as outliers, even though these differences became relatively minor. In contrast to what was found with the linear least-squares method, the robust methods resulted in differences in n values for the water-limited catchments (Fig. 2c, differences between blue and red points) that are generally bigger than the differences in n values for the

energy-limited catchments (Fig. 2b, differences between blue and red points).

The above results clearly show that the projection used to fit the Budyko curve leads to different n values. Hence, n values that are found by fitting Budyko-type curves include a rather high uncertainty, and the interpretation should be carried out with care. This does not necessarily lead to large issues when n values are considered a characteristic for one single catchment (e.g., Zhang et al., 2001; Donohue et al., 2012; Roderick and Farquhar, 2011), as the equations can be solved analytically when just one data point is considered. However, the two formulations of the curve (Eqs. 2 and 3) stem from the same original equation (Eq. 1), meaning that the definition and value of the parameter should, in principle, not change when projections are changed. For this reason, the different values of the n parameter found here for the different projections express an additional uncertainty due to the choice of projection. When a Budyko curve is fit to multiple catchments and the resulting n values are used for interpretation, this additional uncertainty should be considered.

3.2 Distances to the curve and envelopes

Once a Budyko curve is fit to the data, the distance to this curve is often used as a metric for catchment analysis (e.g., Potter et al., 2005; Yokoo et al., 2008; Williams et al., 2012) and supposed to tell something about the state of the catchment, catchment characteristics or the local climate. However, the distance to the curve strongly changed depending on the projection, and the differences in distances depended on the aridity of the catchments (Fig. 3a). For energy-limited catchments ($E_p/P \leq 1$), the distances to the curve were lower for the projection with a wetness index in comparison with the projection with a dryness index (i.e., catchments plot left of the 1 : 1 line in Fig. 3a), whereas the opposite was true for the water-limited catchments (right of the 1 : 1 line in Fig. 3a). This was also more generally confirmed when random samples in the Budyko space were used; see Supplement S2. The distances to the physical boundaries are less often used as a metric for catchment analysis, but these changed similarly (Fig. 3b).

These findings imply as well that exchanging projections of the Budyko curve is not as straightforward as it seems and may result in different outcomes. Moreover, different interpretations can be given to these distances, as an increased distance to $E/E_p = 1$ indicates a decreased energy use efficiency, whereas an increased distance to $E/P = 1$ indicates a decreased rain use efficiency by evaporation. In the literature, several studies focus on explaining these distances to the curve (e.g., Donohue et al., 2007, 2010; Xiong and Guo, 2012; Fang et al., 2016), rather than the n values, but usually only consider one specific projection. Thus, one needs to be aware that these explanations are only valid for that specific projection because the meaning, as well as the value of these distances, changes for a different projection.

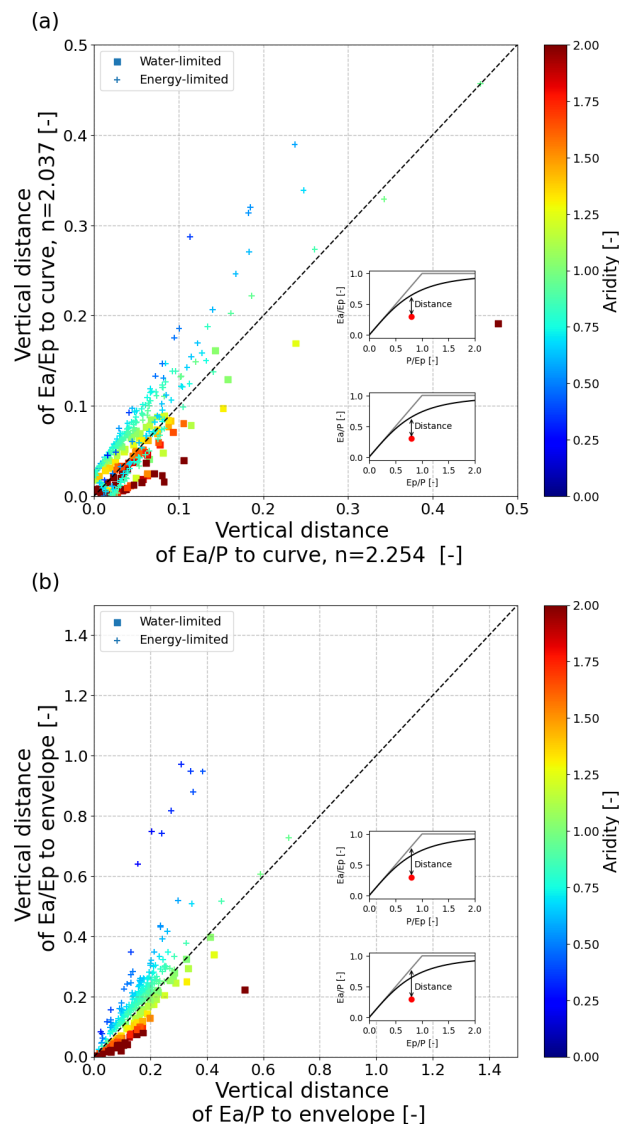


Figure 3. Vertical distances to (a) the envelope of the physical limits of the Budyko framework and (b) vertical distances to the fitted Budyko curve, both for projections normalized by precipitation (x axes) and potential evaporation (y axes). Water-limited catchments ($E_p/P > 1$) are shown by stars, whereas energy-limited catchments are shown by crosses. The color scale indicates the aridity of the catchments.

Therefore, also here a consistent use of the framework is needed. As an aridity of 1.0 introduces a clear distinction between under- and overestimating the distances to the curve and envelope in Fig. 3a and b, one may consider using only the side of the curve with $E_p/P > 1.0$ in the dryness index projection or $P/E_p < 1.0$ in the wetness index projection. In this way, the contracted side of the curve is not used, which could lead to errors due to seemingly low absolute deviations that are in relative terms clearly present.

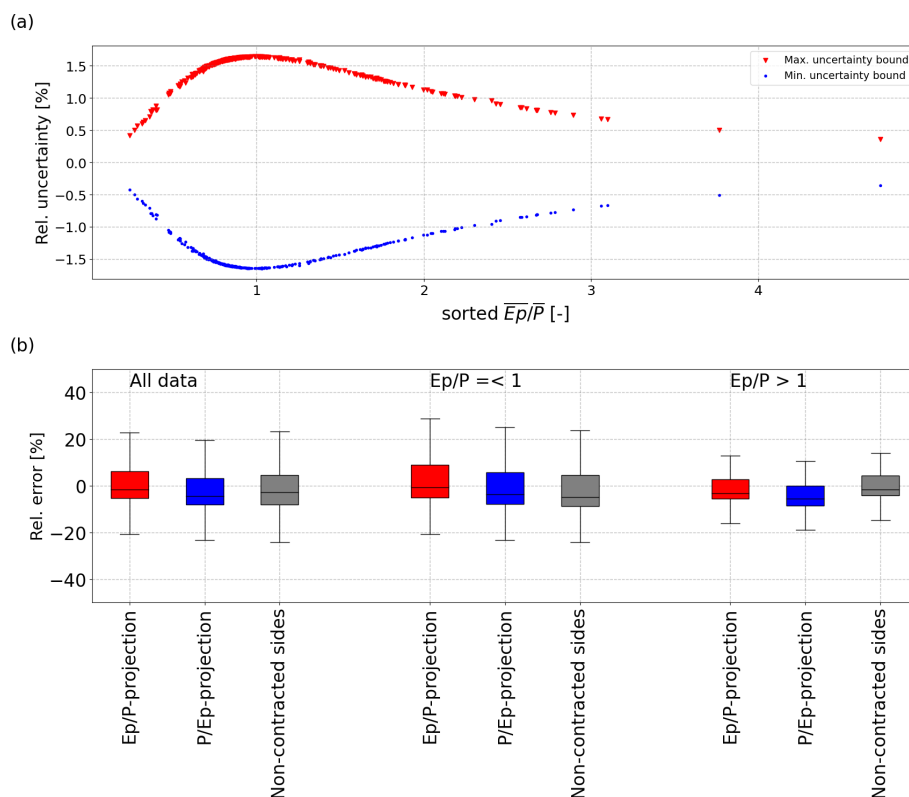


Figure 4. Uncertainty bounds of predicted values of E_a , due to different projections (a). The uncertainty is defined as the relative difference from the expected value of E_a , which is the mean of the predicted values in the two different projections. The relative errors compared with observed (water balance) E_a are shown in (b) for a dryness index projection (red), a wetness index projection (blue) and when only the non-contracted sides of the framework are used (gray). Note that for the blue and red boxplots, the full data are always used to derive the curve, whereas the gray boxplots only used the non-contracted side of the curve. For the gray boxplot with “All data”, the non-contracted sites were used as well; i.e., the curve was fit for catchments with $E_p/P \leq 1$ in a wetness index projection and for catchments with $E_p/P > 1$ in a dryness index projection.

3.3 Uncertainty in predictions

The Budyko framework is often used to predict values of E_a for ungauged catchments, but the uncertainty in predictions of E_a due to the projection used exceeded 1.5 % for catchments with an aridity around 1.0 (Fig. 4a). In addition, the relative error compared with the observed E_a was especially large for energy-limited catchments of the CAMELS dataset ($E_p/P \leq 1$, Fig. 4b). However, the differences in the relative errors between the dryness and wetness index based estimates remained rather small (Fig. 4b).

The uncertainty in predicted values of E_a due to the choice of projection in the Budyko framework has not received much attention to date. Uncertainty evaluations do exist for the Budyko framework or derivatives thereof (e.g., Yang et al., 2014), but these studies did not consider the influence of different projections. Only Andréassian and Perrin (2012) noted that the chosen projection may lead to ambiguities, especially related to leaky or gaining catchments. Implicitly, others may include the projection-related uncertainty indirectly by defining the curves in a more statistical way (Greve

et al., 2015), but we would still argue that the influence of the projection used needs more consideration.

3.4 Influence of outliers

An important cause of the different n values in the different projections are data points that appear as outliers in one projection but not in the other projection. For example, several data points have short vertical distances to the envelope in a dryness index projection but have large distances to the envelope in a wetness index projection and could be considered as outliers (red points in Fig. 5a and b). Vice versa, one data point appears as an outlier in a dryness-index-based projection (blue point in Fig. 5a), but this is not apparent in the other projection (Fig. 5b).

The outliers also influenced the relative errors when the curve was used to predict E_a . The group of catchments identified as outliers in a wetness index projection (i.e., red points in Fig. 5) led to lower n values with a lower curve (see also Fig. 1) and a predicted E_a that is more often underestimated (blue boxes in Fig. 4 shifted downwards). Once only

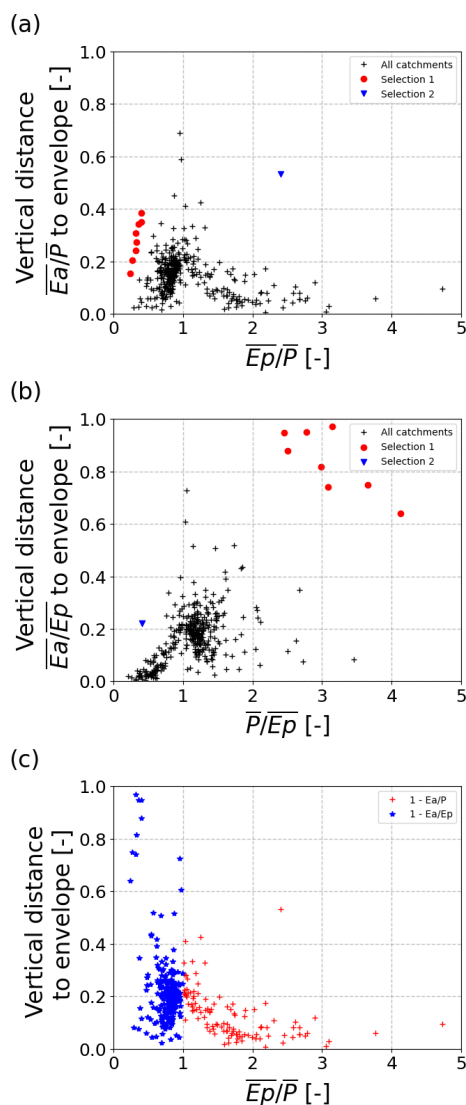


Figure 5. Vertical distances to the envelope for a projection with a dryness index (a) and a wetness index (b), with the same selection in catchments in blue triangles, red dots and black crosses. Distances to the envelope are shown in (c) as a function of the dryness index, with the distances to the non-contracted side in a projection with a dryness index in red (i.e., $E_p/P > 1.0$ with distances $1 - E_a/P$) and the distances to the non-contracted side in a projection with a wetness index in blue (i.e., $P/E_p > 1$ with distances $1 - E_a/E_p$).

the non-contracted side of the framework was used for predictions, the relative errors became either more negative (for $E_p/P \leq 1$) or improved and approached 0 (for $E_p/P > 1$). However, this was merely a result of the absence of the group of outliers (with $E_p/P \leq 1$) for the predictions of the catchments with $E_p/P > 1$. Thus, using only the contracted sides of the framework does not necessarily improve predictions of E_a . Nevertheless, we would still argue that plotting the framework in the two projections and, at least, inspecting the

non-contracted sides for outliers is a valuable and necessary step in Budyko applications.

4 Conclusions

The Budyko framework was applied to a selection of catchments across the contiguous United States, with two different ways to plot the framework. The first projection used a wetness index, whereas the second projection used a dryness index. First, curves were fit with a standard linear least-squares algorithm, followed by more robust methods afterwards. Distances of individual catchments to the curves and envelopes were determined, in order to assess the effects of the different projections. In the next step, we assessed the uncertainty in predicted values of actual evaporation due to the different projections.

In this way, we gained the following insights:

- The differences in n values due to the projection used were ± 0.2 for this dataset (Fig. 1).
- Robust fitting algorithms reduced the differences in n values in the different projections, but differences were still present (Fig. 2).
- The distances to the curve had a systematic dependence on the projection, with larger differences for the non-contracted side of the framework, i.e., $E_p/P > 1$ for the projection with a dryness index and $P/E_p > 1$ for the projection with a wetness index (Fig. 3).
- The resulting uncertainty in predicted values of E_a , solely due to the projections used, could exceed 1.5 % (Fig. 4).
- Data points can appear as outliers in one projection but not in the other, causing differences in the fitting of the curves (Fig. 5).

These findings show that the projection used needs to be considered carefully. Here, we would like to argue to assess always the non-contracted side of the framework in the two projections. Catchments that seem close to the curve and the limits on the contracted side can easily appear as strong outliers on the non-contracted side of the framework, as the absolute value of the relative errors changes on the x axis on the contracted side (i.e., a 10 % error in E_a/P for $E_p/P = 0.5$ differs in absolute terms for $E_p/P = 0.7$). In contrast, this does not happen when only the non-contracted side is considered. At least, it must be noted and considered that the projection used does lead to differences and adds uncertainty to analyses where Budyko curves are fit to multiple catchments. Studies that use Budyko-type curves should therefore assess whether their results are robust and remain unchanged when the projection is changed.

Code and data availability. The full analysis, including all scripts and data, is available on Renku (<https://renkulab.io/projects/remko.nijzink/budyko>, Nijzink and Schymanski, 2022a; <https://doi.org/10.5281/zenodo.7068888>, Nijzink and Schymanski, 2022b).

Supplement. The supplement related to this article is available online at: <https://doi.org/10.5194/hess-26-4575-2022-supplement>.

Author contributions. Analyses, preprocessing and post-processing of data were carried out by RCN. SJS and RCN contributed to the final text.

Competing interests. At least one of the (co-)authors is a member of the editorial board of *Hydrology and Earth System Sciences*. The peer-review process was guided by an independent editor, and the authors also have no other competing interests to declare.

Disclaimer. Publisher's note: Copernicus Publications remains neutral with regard to jurisdictional claims in published maps and institutional affiliations.

Acknowledgements. This study is part of the WAVE project, funded by the Luxembourg National Research Fund (FNR) ATTRACT programme (A16/SR/11254288). We thank NCAR for making the CAMELS data available (<https://ral.ucar.edu/solutions/products/camels>, last access: 9 February 2022).

Financial support. This research has been supported by the Fonds National de la Recherche Luxembourg (FNR) ATTRACT programme (grant no. A16/SR/11254288).

Review statement. This paper was edited by Adriaan J. (Ryan) Teuling and reviewed by two anonymous referees.

References

- Addor, N., Newman, A. J., Mizukami, N., and Clark, M. P.: The CAMELS data set: catchment attributes and meteorology for large-sample studies, *Hydrol. Earth Syst. Sci.*, 21, 5293–5313, <https://doi.org/10.5194/hess-21-5293-2017>, 2017.
- Andréassian, V. and Perrin, C.: On the ambiguous interpretation of the Turc-Budyko nondimensional graph, *Water Resour. Res.*, 48, W10601, <https://doi.org/10.1029/2012WR012532>, 2012.
- Andréassian, V. and Sari, T.: Technical Note: On the puzzling similarity of two water balance formulas – Turc–Mezentsev vs. Tixeront–Fu, *Hydrol. Earth Syst. Sci.*, 23, 2339–2350, <https://doi.org/10.5194/hess-23-2339-2019>, 2019.
- Andréassian, V., Mander, U., and Pae, T.: The Budyko hypothesis before Budyko: The hydrological legacy of Evald Oldekop, *J. Hydrol.*, 535, 386–391, <https://doi.org/10.1016/j.jhydrol.2016.02.002>, 2016.
- Bouaziz, L. J. E., Aalbers, E. E., Weerts, A. H., Hegnauer, M., Buiteveld, H., Lammersen, R., Stam, J., Sprokkereef, E., Savenije, H. H. G., and Hrachowitz, M.: Ecosystem adaptation to climate change: the sensitivity of hydrological predictions to time-dynamic model parameters, *Hydrol. Earth Syst. Sci.*, 26, 1295–1318, <https://doi.org/10.5194/hess-26-1295-2022>, 2022.
- Budyko, M.: *Climate and Life*, Academic Press, New York and London, english Edited by Miller, D. H., ISBN 9780121394509, 1974.
- Choudhury, B.: Evaluation of an empirical equation for annual evaporation using field observations and results from a biophysical model, *J. Hydrol.*, 216, 99–110, [https://doi.org/10.1016/S0022-1694\(98\)00293-5](https://doi.org/10.1016/S0022-1694(98)00293-5), 1999.
- Coron, L., Andréassian, V., Perrin, C., and Le Moine, N.: Graphical tools based on Turc-Budyko plots to detect changes in catchment behaviour, *Hydrolog. Sci. J.*, 60, 1394–1407, <https://doi.org/10.1080/02626667.2014.964245>, 2015.
- Donohue, R., Roderick, M., and McVicar, T.: Can dynamic vegetation information improve the accuracy of Budyko's hydrological model?, *J. Hydrol.*, 390, 23–34, <https://doi.org/10.1016/j.jhydrol.2010.06.025>, 2010.
- Donohue, R. J., Roderick, M. L., and McVicar, T. R.: On the importance of including vegetation dynamics in Budyko's hydrological model, *Hydrol. Earth Syst. Sci.*, 11, 983–995, <https://doi.org/10.5194/hess-11-983-2007>, 2007.
- Donohue, R. J., Roderick, M. L., and McVicar, T. R.: Roots, storms and soil pores: Incorporating key ecohydrological processes into Budyko's hydrological model, *J. Hydrol.*, 436–437, 35–50, <https://doi.org/10.1016/j.jhydrol.2012.02.033>, 2012.
- Dooge, J. C. I., Bruen, M., and Parmentier, B.: A simple model for estimating the sensitivity of runoff to long-term changes in precipitation without a change in vegetation, *Adv. Water Resour.*, 23, 153–163, 1999.
- Fang, K., Shen, C., Fisher, J. B., and Niu, J.: Improving Budyko curve-based estimates of long-term water partitioning using hydrologic signatures from GRACE, *Water Resour. Res.*, 52, 5537–5554, <https://doi.org/10.1002/2016WR018748>, 2016.
- Fu, B.: On the calculation of the evaporation from land surface, *Sci. Atmos. Sin.*, 5, 23–31, 1981 (in Chinese).
- Gnann, S. J., Woods, R. A., and Howden, N. J. K.: Is There a Baseflow Budyko Curve?, *Water Resour. Res.*, 55, 2838–2855, <https://doi.org/10.1029/2018WR024464>, 2019.
- Greve, P., Gudmundsson, L., Orłowsky, B., and Seneviratne, S. I.: Introducing a probabilistic Budyko framework, *Geophys. Res. Lett.*, 42, 2261–2269, <https://doi.org/10.1002/2015GL063449>, 2015.
- Greve, P., Burek, P., and Wada, Y.: Using the Budyko Framework for Calibrating a Global Hydrological Model, *Water Resour. Res.*, 56, e2019WR026280, <https://doi.org/10.1029/2019WR026280>, 2020.
- Hulsman, P., Bogaard, T. A., and Savenije, H. H. G.: Rainfall-runoff modelling using river-stage time series in the absence of reliable discharge information: a case study in the semi-arid Mara River basin, *Hydrol. Earth Syst. Sci.*, 22, 5081–5095, <https://doi.org/10.5194/hess-22-5081-2018>, 2018.

- Levenberg, K.: A method for the solution of certain non-linear problems in least squares, *Q. Appl. Math.*, 2, 164–168, <https://doi.org/10.1090/qam/10666>, 1944.
- Li, D., Pan, M., Cong, Z., Zhang, L., and Wood, E.: Vegetation control on water and energy balance within the Budyko framework, *Water Resour. Res.*, 49, 969–976, <https://doi.org/10.1002/wrcr.20107>, 2013.
- Liang, W., Bai, D., Wang, F., Fu, B., Yan, J., Wang, S., Yang, Y., Long, D., and Feng, M.: Quantifying the impacts of climate change and ecological restoration on stream-flow changes based on a Budyko hydrological model in China's Loess Plateau, *Water Resour. Res.*, 51, 6500–6519, <https://doi.org/10.1002/2014WR016589>, 2015.
- Mezentsev, V. S.: More on the calculation of average total evaporation, *Meteorol. Gidrol.*, 5, 24–26, 1955.
- Mianabadi, A., Coenders-Gerrits, M., Shirazi, P., Ghahraman, B., and Alizadeh, A.: A global Budyko model to partition evaporation into interception and transpiration, *Hydrol. Earth Syst. Sci.*, 23, 4983–5000, <https://doi.org/10.5194/hess-23-4983-2019>, 2019.
- Moussa, R. and Lhomme, J.-P.: The Budyko functions under non-steady-state conditions, *Hydrol. Earth Syst. Sci.*, 20, 4867–4879, <https://doi.org/10.5194/hess-20-4867-2016>, 2016.
- Newman, A. J., Clark, M. P., Sampson, K., Wood, A., Hay, L. E., Bock, A., Viger, R. J., Blodgett, D., Brekke, L., Arnold, J. R., Hopson, T., and Duan, Q.: Development of a large-sample watershed-scale hydrometeorological data set for the contiguous USA: data set characteristics and assessment of regional variability in hydrologic model performance, *Hydrol. Earth Syst. Sci.*, 19, 209–223, <https://doi.org/10.5194/hess-19-209-2015>, 2015.
- Nijzink, R. C. and Schymanski, S. J.: The role of vegetation optimality in the Budyko framework, *Renku [code] and [data set]*, <https://renkulab.io/projects/remko.nijzink/budyko>, last access: 7 September 2022a.
- Nijzink, R. and Schymanski, S.: The role of vegetation optimality in the Budyko framework, *Zenodo [data set]*, <https://doi.org/10.5281/zenodo.7068888>, 2022b.
- Nijzink, R. C., Almeida, S., Pechlivanidis, I. G., Capell, R., Gustafssons, D., Arheimer, B., Parajka, J., Freer, J., Han, D., Wagener, T., van Noijen, R. R. P., Savenije, H. H. G., and Hrachowitz, M.: Constraining Conceptual Hydrological Models With Multiple Information Sources, *Water Resour. Res.*, 54, 8332–8362, <https://doi.org/10.1029/2017WR021895>, 2018.
- Ning, T., Li, Z., and Liu, W.: Vegetation dynamics and climate seasonality jointly control the interannual catchment water balance in the Loess Plateau under the Budyko framework, *Hydrol. Earth Syst. Sci.*, 21, 1515–1526, <https://doi.org/10.5194/hess-21-1515-2017>, 2017.
- Ol'Dekop, E.: On evaporation from the surface of river basins, *Trans. Meteorol. Obs.*, 4, 200, 1911.
- Oudin, L., Andréassian, V., Lerat, J., and Michel, C.: Has land cover a significant impact on mean annual streamflow? An international assessment using 1508 catchments, *J. Hydrol.*, 357, 303–316, <https://doi.org/10.1016/j.jhydrol.2008.05.021>, 2008.
- Pike, J.: The estimation of annual run-off from meteorological data in a tropical climate, *J. Hydrol.*, 2, 116–123, [https://doi.org/10.1016/0022-1694\(64\)90022-8](https://doi.org/10.1016/0022-1694(64)90022-8), 1964.
- Porporato, A.: Hydrology without dimensions, *Hydrol. Earth Syst. Sci.*, 26, 355–374, <https://doi.org/10.5194/hess-26-355-2022>, 2022.
- Potter, N. J., Zhang, L., Milly, P. C. D., McMahon, T. A., and Jakeman, A. J.: Effects of rainfall seasonality and soil moisture capacity on mean annual water balance for Australian catchments, *Water Resour. Res.*, 41, W06007, <https://doi.org/10.1029/2004WR003697>, 2005.
- Roderick, M. L. and Farquhar, G. D.: A simple framework for relating variations in runoff to variations in climatic conditions and catchment properties, *Water Resour. Res.*, 47, W00G07, <https://doi.org/10.1029/2010WR009826>, 2011.
- A. Sankarasubramanian, Wang, D., Archfield, S., Reitz, M., Vogel, R. M., Mazrooei, A., and Mukhopadhyay, S.: HESS Opinions: Beyond the long-term water balance: evolving Budyko's supply–demand framework for the Anthropocene towards a global synthesis of land-surface fluxes under natural and human-altered watersheds, *Hydrol. Earth Syst. Sci.*, 24, 1975–1984, <https://doi.org/10.5194/hess-24-1975-2020>, 2020.
- Schreiber, P.: Über die Beziehungen zwischen dem Niederschlag und der Wasserführung der Flüsse in Mitteleuropa, *Z. Meteorol.*, 21, 441–452, 1904.
- Shao, Q., Traylen, A., and Zhang, L.: Nonparametric method for estimating the effects of climatic and catchment characteristics on mean annual evapotranspiration, *Water Resour. Res.*, 48, W03517, <https://doi.org/10.1029/2010WR009610>, 2012.
- Turc, L.: Calcul du bilan de l'eau: évaluation en fonction des précipitations et des températures, *IAHS-AISH P.*, 37, 88–200, 1954.
- van der Velde, Y., Vercauteren, N., Jaramillo, F., Dekker, S. C., Destouni, G., and Lyon, S. W.: Exploring hydroclimatic change disparity via the Budyko framework, *Hydrol. Process.*, 28, 4110–4118, <https://doi.org/10.1002/hyp.9949>, 2014.
- Wang, F., Xia, J., Zou, L., Zhan, C., and Liang, W.: Estimation of time-varying parameter in Budyko framework using long short-term memory network over the Loess Plateau, China, *J. Hydrol.*, 607, 127571, <https://doi.org/10.1016/j.jhydrol.2022.127571>, 2022.
- Williams, C. A., Reichstein, M., Buchmann, N., Baldocchi, D., Beer, C., Schwalm, C., Wohlfahrt, G., Hasler, N., Bernhofer, C., Foken, T., Papale, D., Schymanski, S., and Schaefer, K.: Climate and vegetation controls on the surface water balance: Synthesis of evapotranspiration measured across a global network of flux towers, *Water Resour. Res.*, 48, W06523, <https://doi.org/10.1029/2011WR011586>, 2012.
- Xiong, L. and Guo, S.: Appraisal of Budyko formula in calculating long-term water balance in humid watersheds of southern China, *Hydrol. Process.*, 26, 1370–1378, <https://doi.org/10.1002/hyp.8273>, 2012.
- Yang, D., Shao, W., Yeh, P. J.-F., Yang, H., Kanae, S., and Oki, T.: Impact of vegetation coverage on regional water balance in the nonhumid regions of China, *Water Resour. Res.*, 45, W00A14, <https://doi.org/10.1029/2008WR006948>, 2009.
- Yang, H., Yang, D., Lei, Z., and Sun, F.: New analytical derivation of the mean annual water-energy balance equation, *Water Resour. Res.*, 44, W03410, <https://doi.org/10.1029/2007WR006135>, 2008.
- Yang, H., Yang, D., and Hu, Q.: An error analysis of the Budyko hypothesis for assessing the contribution of cli-

- mate change to runoff, *Water Resour. Res.*, 50, 9620–9629, <https://doi.org/10.1002/2014WR015451>, 2014.
- Yang, H., Xiong, L., Xiong, B., Zhang, Q., and Xu, C.-Y.: Separating runoff change by the improved Budyko complementary relationship considering effects of both climate change and human activities on basin characteristics, *J. Hydrol.*, 591, 125330, <https://doi.org/10.1016/j.jhydrol.2020.125330>, 2020.
- Yokoo, Y., Sivapalan, M., and Oki, T.: Investigating the roles of climate seasonality and landscape characteristics on mean annual and monthly water balances, *J. Hydrol.*, 357, 255–269, <https://doi.org/10.1016/j.jhydrol.2008.05.010>, 2008.
- Zhang, L., Dawes, W. R., and Walker, G. R.: Response of mean annual evapotranspiration to vegetation changes at catchment scale, *Water Resour. Res.*, 37, 701–708, <https://doi.org/10.1029/2000WR900325>, 2001.
- Zhao, J., Huang, S., Huang, Q., Leng, G., Wang, H., and Li, P.: Watershed water-energy balance dynamics and their association with diverse influencing factors at multiple time scales, *Sci. Total Environ.*, 711, 135189, <https://doi.org/10.1016/j.scitotenv.2019.135189>, 2020.